Correlated Magnetic Tail and Radiation Belt Observations

by

Norman F. Ness
NASA-Goddard Space Flight Center

and

Donald J. Williams
Applied Physics Laboratory-Johns Hopkins Univ.

[redacted]

July 1965

Correlated Magnetic Tail and Radiation Belt Observations

The NASA IMP-I or Explorer XVIII satellite has provided measurements of magnetic field strengths and directions out to a geocentric distance of 31.5 R_e (earth radii). As a result, the earth's magnetic field has been mapped out in great detail[1,2] in both the solar and anti-solar directions. During the period of these measurements, (Nov. 1963-May 1964) the APL satellite 1963 38C was sampling the trapped electron population at an altitude of 1100 Km[3,4]. The purpose of this note is to report simultaneous observations from the above two satellites during a magnetic disturbance in April 1964 showing the interplay between the earth's magnetic tail and the radiation belts within the magnetosphere.

The sensors and satellites have been described previously[1,3]. Briefly, satellite 1963 38C is a magnetically oriented satellite in a very nearly circular polar orbit at an altitude of 1100 Km. The detector of interest is a 1000μ surface barrier solid state detector monitoring trapped electrons of energy $\geq$ 280 Kev. During the time of the measurements being reported, the orbital plane of 1963 38C was within 4^o of the noon-midnight meridian.

The orbit of the IMP-I satellite is highly eccentric so that for 80% of the orbital period (93.5 hrs) the spacecraft is located well beyond 10 R_e, $\approx$ 64000 Km. At the time of the magnetic disturbance IMP-I was approaching apogee of it 33rd orbit. The angle to the Earth-Sun line of the line of apsides was 148° West of the Sun, corresponding to a local time of 0200.

Beyond the trapping region in the anti-solar direction the field topology as measured by Ness[2] has revealed a remarkable tail-like structure geometrically similar to the tail of a comet. It contains a region of small or zero magnetic field strength (neutral sheet) separating solar directed fields in the northern hemisphere from anti-solar directed fields in the southern hemisphere. Such a topology requires that the neutral sheet be filled with a plasma of sufficient energy to maintain the separate regions of oppositely directed magnetic fields. These experimental results are in agreement with the theoretical suggestions of Piddington[5], Axford et. al.,[6] and Dessler[7] regarding the interaction of the solar wind with the geomagnetic field leading to the formation of the earth's magnetic tail. A recent analysis[8] has shown that the spatial distribution of energetic ($E_e \geq 280$ kev) trapped electrons in the outer radiation zone during magnetically quiet periods is consistent with their movement in a distorted field as described above, under conservation of the adiabatic invariants.

We now present observations which indicate that during a magnetic storm the midnight latitude profile of trapped electrons at 1100 Km behaves in a manner consistent with the behavior of the magnetic tail field at $\approx 30\ R_e$. The terrestrial magnetic disturbance of interest begins at 1525 UT on April 1, 1964 and was identified as a sudden commencement[9]. It is shown in Figure 1 as measured by the horizonal component at a number of world wide stations with simultaneous graphs of the magnitude $\bar{F}$ and two angles θ and ϕ defining the vector magnetic tail field in solar ecliptic coordinates[1]. Note that $\theta = 0^o$, $\phi = 180^o$ corresponds to the anti-solar direction.

Subsequent to the initial phase, the main phase decrease of the geomagnetic storm is observed during the next 8 hours. At the time of the decrease of the terrestrial field, the tail field increases significantly and in general in remarkable time correlation with the finer details of the ground data. We interpret this as the first experimental evidence of the important role played by the earth's magnetic tail in geomagnetic storm phenomena[5]. Additional lines of force originating in the polar cap regions are extended into the earth's tail, thereby causing the observed anti-correlation of terrestrial and tail fields. Note that the terrestrial data have been processed with numerical filters[10] to remove the classical diurnal harmonics, S_q. and therefore each station trace is approximately a local disturbance field, D_{st}.

In Figure 2 we show the four nightside passes from 1963 38C during the period Mar. 31, 1964 to 2 April 1964. Passes a and b, obtained prior to the disturbance, display very similar quiet-time profiles. Pass c was obtained just after the height of the disturbance and shows a distinct collapse of the outer boundary to lower latitudes. Note also that no new particles have been added at this time. Pass d, taken ~6 hrs after the height of the disturbance, shows that the outer boundary has moved back toward the pre-storm value and that new particles have now been added.

The collapse of the outer boundary to lower latitudes, as shown in Figure 2, can be interpreted to be the result of formerly closed field lines being extended into the tail during the magnetic disturbance. This interpretation is strengthened by the observation, shown in Figure 1, that the magnetic field in the tail increases in magnitude during the magnetic disturbance. As the field line orientation does not change, such an increase in magnitude requires an increase in plasma density within the neutral sheet, which in turn will extend formerly closed lines of force out into the tail field region. Particles trapped on these field lines will be thus injected into the distant magnetic field, possibly forming some of the electron "islands" observed recently in these regions[11].

Using the tail field model constructed by Williams and Mead[8] for fitting the energetic trapped electron spatial distribution and assuming adiabatic invariant conservation, we are able to quantitatively obtain the midnight trapping boundary. This is defined by analysis of field line closure obtained by substituting into the field model the appropriate values of the tail field as shown in Figure 1. Figure 3 shows the measured field variations along with the expected trapping boundary variations on the midnight meridian.

For this analysis, averages of the tail field over an interval of 3 hours were computed so that a direct comparison with the planetary magnetic index K_p could be made, as shown in Figure 3. Strong correlation between the magnitude of the tail field and K_p is significant in that high fields correspond to high K_p and vice versa. The 3 hour interval also appears to be a reasonable time scale to consider as required for the readjustment of the magnetosphere and radiation belts in response to the tail field changes. In this model the following current sheet parameters were used: inner edge, 8 R_e; outer edge, 200 R_e and field strengths as shown in Figure 3.

The measured trapping boundaries, shown as vertical arrows in Figure 2, are identified in Figure 3 as a, b, c and d.

While the absolute position of the expected and measured trapping boundaries differ by an average of about five degrees, it is seen that the magnitude of the boundary collapse during the disturbance can be explained by the behavior of the tail field. The discrepancy in the absolute position has been noted and discussed previously[8]. Possible explanations include, the use of a more appropriate current sheet in the model, the effects of a possible ring current, a readjustment of the coefficients defining the field due to the boundary currents, and the fact that a trapping boundary defined at a lower count rate would produce slightly higher cutoff latitudes.

The motion of trapping boundaries to lower latitudes during magnetic disturbances has been noted previously[12, 4]. Here we have shown using a tail field model of the magnetosphere and assuming motion of charged particles conserving the adiabatic invariants that the behavior of the radiation cavity as observed at 1100km is consistent with the measured behavior of the magnetic field some 30 R_e in the tail. Moreover, the magnitude of the latitude shift is in fair quantitative agreement with the results of a field model using a tail like structure.

Acknowledgements

We wish to express our appreciation to: Dr. G.D. Mead for performing the magnetic field calculations, and Mr. K.W. Behannon for performing the terrestrial magnetogram analysis.

References

1. N. F. Ness, C. S. Scearce, and J. B. Seek, J. Geophys. Res. 69, 3531 (1964)
2. N. F. Ness, J. Geophys. Res. 70, 2989 (1965)
3. D. J. Williams and A. M. Smith, J. Geophys. Res. 70, 541 (1965)
4. D. J. Williams and W. F. Palmer, J. Geophys. Res. 70, 557 (1965)
5. J. H. Piddington, J. Geophys. Res. 65, 93 (1960)
6. W. I. Axford, H. E. Petschek, and G. L. Siscoe, J. Geophys. Res., 70, 1231 (1965)
7. A. J. Dessler, J. Geophys. Res 69, 3913 (1964)
8. D. J. Williams and G. D. Mead, J. Geophys. Res 70, 3017 (1965)
9. J. V. Lincoln, J. Geophys. Res. 70, 2233 (1965)
10. K. W. Behannon and N. F. Ness, NASA Tech. Note, to appear (1965)
11. K. A. Anderson, H. K. Harris, and R. J. Paoli, J. Geophys. Res. 70, 1039 (1965)
12. B. Maehlum and B. J. O'Brien, J. Geophys. Res. 68, 997 (1963)

Figure Captions

1. Sudden commencement geomagnetic storm of April 1, 1964. Correlated IMP-I satellite measurements at a geocentric distance of approximately 180,000 Km are compared to the horizontal component of the terrestrial magnetic field (See text).

2. Measured particle flux intensity on satellite 1963 38C during sudden commencement storm of April 1, 1964. Vertical arrows indicate identified boundary of trapping region. Plotted are trapped electron intensities (true counts per sec.) as function of invariant latitude. Multiplication by 500 yields flux values($\#/cm^2 sec.sr$).

3. Correlation of planetary magnetic index K_p. predicted and observed invariant latitude of boundary of radiation cavity and magnetic tail field. For a discussion of these various phenomena see text.

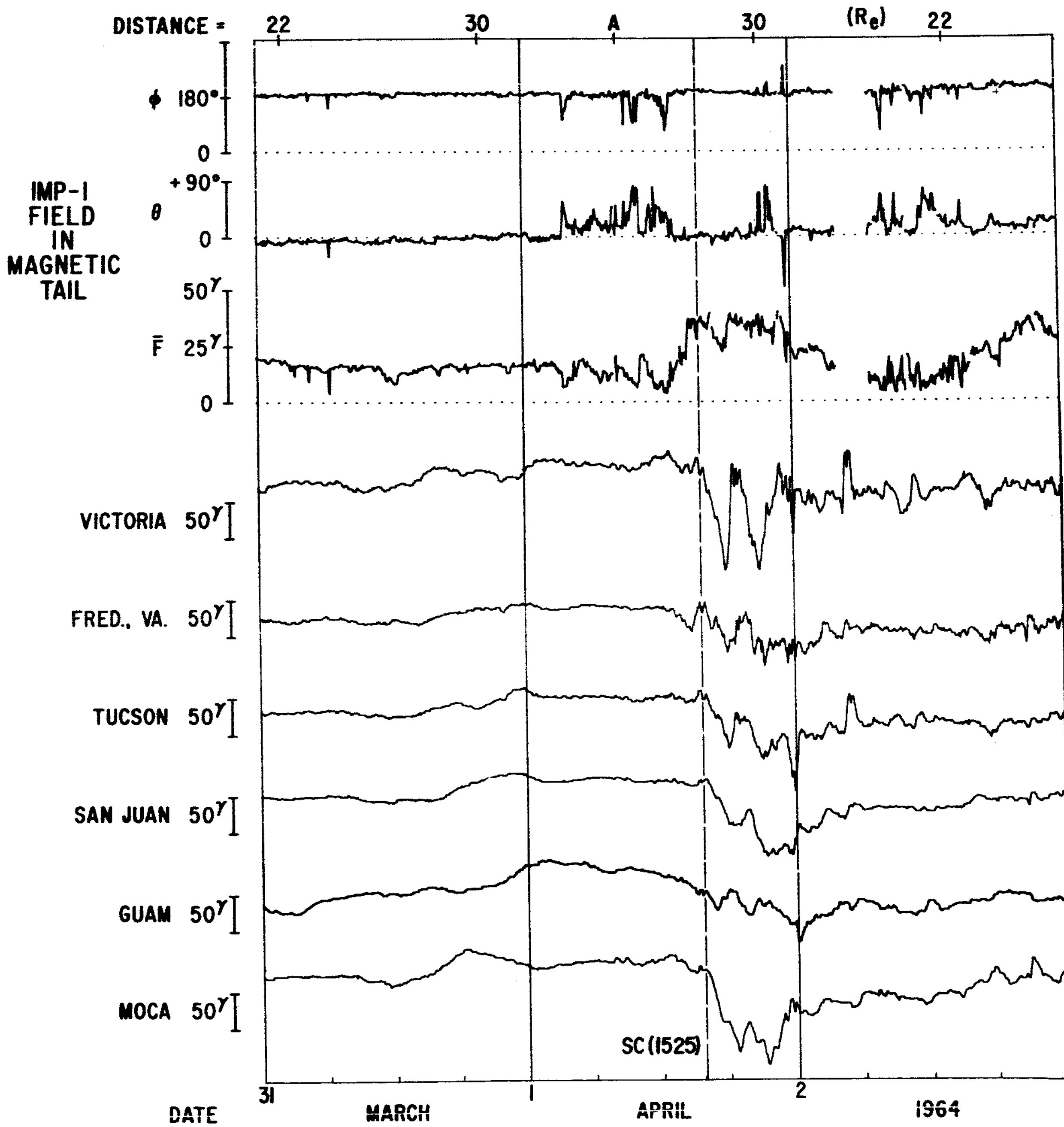
DISTANCE = 22 30 A 30 (Re) 22
IMP-I FIELD IN MAGNETIC TAIL
ϕ 180°
0
θ +90°
0
F̄ 50γ
25γ
0
VICTORIA 50γ
FRED., VA. 50γ
TUCSON 50γ
SAN JUAN 50γ
GUAM 50γ
MOCA 50γ
SC(1525)
DATE 31 MARCH 1 APRIL 2 1964 3

Figure 1

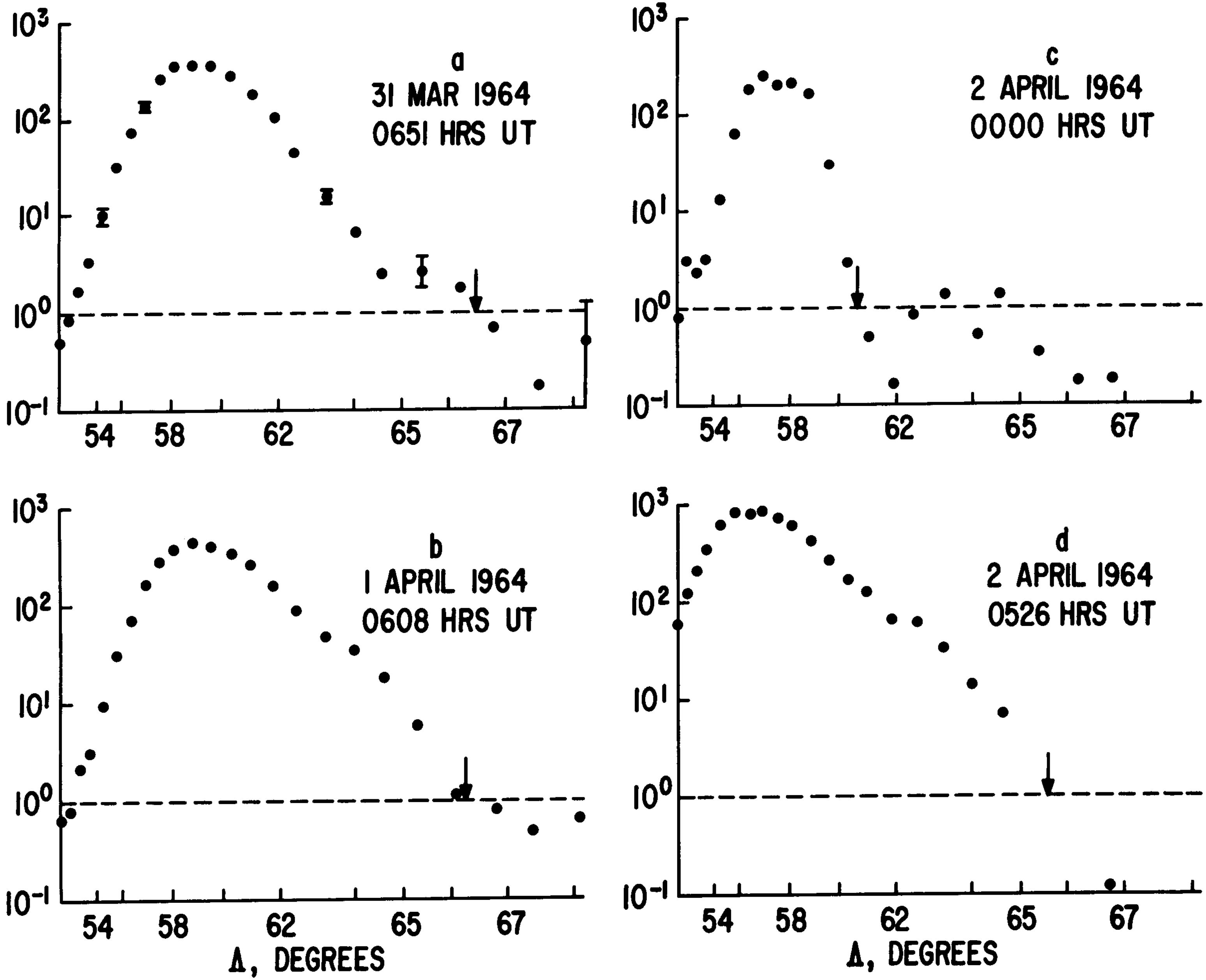
a
31 MAR 1964
0651 HRS UT
c
2 APRIL 1964
0000 HRS UT
b
1 APRIL 1964
0608 HRS UT
d
2 APRIL 1964
0526 HRS UT
10³
10²
10¹
10⁰
10⁻¹
54
58
62
65
67
Λ, DEGREES

Figure 2

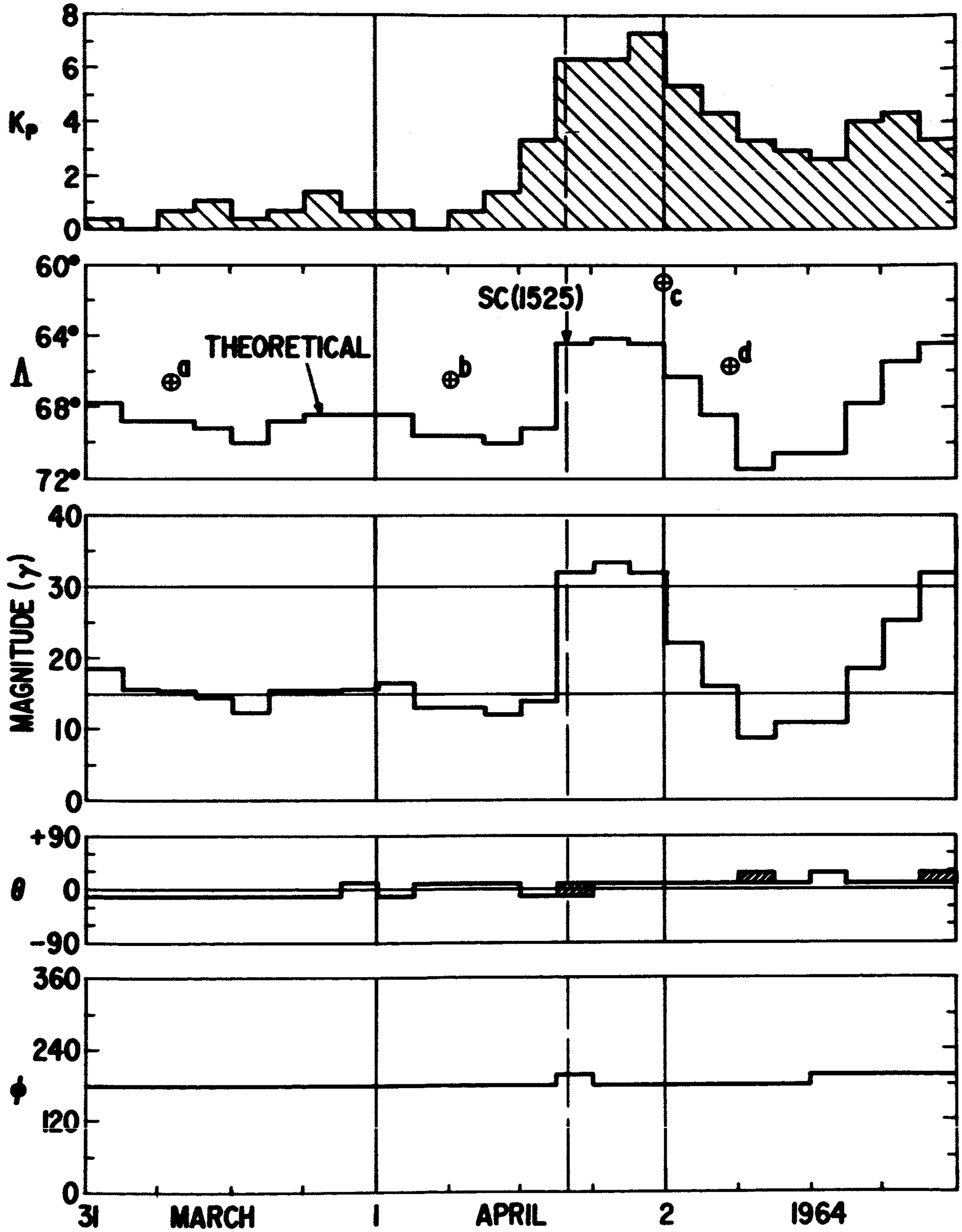

Kp
Λ
THEORETICAL
SC(1525)
⊕a
⊕b
⊕c
⊕d
MAGNITUDE (γ)
θ
φ
31
MARCH
1
APRIL
2
1964

Figure 3